UC San Diego
UC San Diego Previously Published Works

Title
Distribution Profiling of Circulating MicroRNAs in Serum

Permalink
https://escholarship.org/uc/item/21v057h6

Journal
Analytical Chemistry, 86(18)

ISSN
0003-2700

Authors
Ashby, Jonathan
Flack, Kenneth
Jimenez, Luis A
et al.

Publication Date
2014-09-16

DOI
10.1021/ac5028929

Peer reviewed

Distribution profiling of circulating microRNAs in serum

SCHOLARONE™
Manuscripts

Distribution profiling of circulating microRNAs in serum

Jonathan Ashby[1‡], Kenneth Flack[1‡], Luis A. Jimenez[2], Yaokai Duan[1], Abdel-Kareem Khatib[1],

George Somlo[4], Shizhen Emily Wang[5], Xinping Cui[3], Wenwan Zhong[1]*

[1]Department of Chemistry; [2]Program in Biomedical Sciences; [3]Department of Statistics,

University of California, Riverside;

[4]Department of Medical Oncology, [5]Department of Cancer Biology, Beckman Research Institute,

City of Hope Medical Center, Duarte, CA 91010, USA

Keywords: Fractionation, exosomes, lipoprotein particles, cancer biomarkers, circulating microRNA

ABSTRACT

Circulating microRNAs (miRNAs) are potential biomarkers useful in cancer diagnosis. They have been found to be bound to various carriers like proteins, lipoprotein particles, and exosomes. It is likely that only miRNAs in particular carriers, but not the overall quantity, are directly related to cancer development. Herein, we developed a method for rapid separation of different miRNA carriers in serum using asymmetrical flow field flow fractionation (AF4). Sera from two healthy individuals (control) or from two cancer patients (case) were fractionated. Six fractions enriching different types of miRNA carriers, such as the lipoprotein particles and exosomes, were collected. The quantities of eight selected miRNAs in each fraction were obtained by RT-qPCR to yield their distribution profiles among the carriers. Larger changes in miRNA quantity between the control and the case were detected in the fractionated results compared to the sum values. Statistical analysis on the distribution profiles also proved that, the quantities of 4 miRNAs within particular fractions showed significant difference between the controls and the cases. On contrary, if the overall quantity of the miRNA was subject to the same statistical analysis, only 2 miRNAs exhibited significant difference. Moreover, principle component analysis revealed good separation between the controls and the cases with the fractionated miRNA amounts. All in all, we have demonstrated that, our method enables comprehensive screening of the distribution of circulating miRNAs in the carriers. The obtained distribution profile enlarges the miRNA expression difference between healthy individuals and cancer patients, facilitating the discovery of specific miRNA biomarkers for cancer diagnosis.

Early detection of cancer can enhance the survival rate of patients but the success strongly relies on the availability of specific and sensitive biomarkers. One class of promising biomarkers for cancer diagnosis is the microRNAs (miRNAs). They bind to target mRNAs and inhibit translation or induce degradation of target transcripts.[1,2] Overexpression of miRNAs that inhibit the tumor suppressor genes can interfere with the anti-oncogenic pathway; while deletion or epigenetic silencing of miRNAs that target oncogenes can increase oncogenic potency.[3-6] It is also recognized that miRNA profiles more accurately reflect the developmental lineage and tissue origin of human cancers than the mRNA profiles.[7-9] Compared to proteins, miRNAs have simpler structure and less complex post-synthesis processing; and can be detected by the highly sensitive PCR methods. More appealing, miRNAs can be released into the circulation system and stably present at levels detectible by sensitive techniques like RT-PCR.[10-13] Accumulating evidence shows that circulating miRNAs exhibit varied patterns between cancer patients and healthy controls, with the patterns of some secretory miRNAs altered in the early stage of cancer initiation.[14-16] Since sampling from circulating body fluids, like blood, urine, saliva, etc. is considered to be convenient and non-invasive compared to other biopsy methods, more and more research efforts have been devoted to obtaining the comprehensive profiles of circulating miRNAs, and validate their utility as biomarkers.[17,18]

Still, it is a long route from proof-of-principle to creation of reliable and reproducible miRNA clinical tests. One obstacle is that, not all circulating miRNAs are related to cancer development. The cancer-irrelevant miRNAs can be secreted by blood cells; or be shed after cells die. They could then contribute to large variances in miRNA abundances between individuals and subsidize signals from the cancer-related miRNAs during quantification. It has been known that, the cell-free miRNAs are protected from nucleases in extracellular

environments and in body fluids by various types of carriers. The carriers can be proteins like Argonaute (AGO) 2 and GW182[19,20] that belong to the RNA-induced silencing complex (RISC); be the high-density lipoprotein (HDL) particles that could mediate intracellular communication;[21,22] or be vesicles like the exosomes[23-25] which are believed to be one of the exportation routes for miRNAs from malignant cells.[26] While active miRNA secretion by malignant cells could be the consequence of dysregulation of cellular pathways, for-purpose exportation and uptake could be related to tumor progression and metastasis.[27-29] Therefore, to better eliminate the cancer-irrelevant miRNAs and reveal the more specific miRNA markers, isolation of miRNAs from carriers that are specifically secreted by cancer cells could be a solution. Thus, HDL and exosomes have recently been focused in study of circulating miRNAs.

Pure HDL or exosomes are often obtained by ultracentrifugation[20,21,26,30-32] and immunoaffinity capture.[33,34] Ultracentrifugation can provide good size/density resolution; but it requires large sample volumes, is very tedious and time-consuming, and typically renders low recovery. Immunoaffinity capture is easy to perform and provides high specificity, but can only target one type of carriers at a time.[35,36] In the pioneering study of miRNA carriers done by Arroyo *et al.*,[19] serum was fractionated with size exclusion chromatography (SEC) to reveal the existence of the exosomal and exosome-free circulating miRNAs. Vickers *et al.* also applied SEC to further characterize the HDL isolated by ultracentrifugation.[21] However, in SEC, good separation resolution can only be achieved within a small size range; interaction of biomolecules with the column materials is problematic; and integrity of biocomplexes or vesicle structures after passing through the packed column is questionable.

While recovering miRNAs from either pure HDL or exosomes could possibly remove the cancer-irrelevant miRNAs shredded by normal cells, it is actually not conclusive about which

carriers are more important in cancer diagnosis. Thus, study of miRNA distribution among all types of carriers is necessary to answer this question. Compared to SEC and ultracentrifugation, asymmetrical flow field-flow fractionation (AF4) is gentler for better preservation of the binding between miRNAs and their carriers.[37] Due to its non-interactive separation ability, AF4 can be used to isolate intact macromolecular complexes, such as aptamer-protein interactions, antibody-antigen interactions, and protein-drug interactions.[38-40] In addition, AF4 has previously been used for analysis of exosomes in serum.[41-43] Therefore, it is the method of choice for rapid separation of different miRNA carriers based on their hydrodynamic diameters, enabling the screening of miRNA distribution among various carriers. Comparing the distribution profiles obtained from healthy individuals and cancer patients may help to reveal which types of carriers are more relevant to cancer development, and thus enhance the sensitivity and specificity in diagnosis when using the miRNAs enclosed in those carriers as the markers.

Herein, we employed AF4 to fractionate the whole serum. Discrete elution fractions were collected. Total RNAs were extracted from each fraction; and the amounts of 8 selected miRNAs in each fraction were quantified by RT-qPCR. Proteins eluted in each fraction were also extracted and identified to reveal the identities of carriers enriched in each fraction. The distribution profiles acquired from the sera of healthy individuals were compared with those from patients with breast cancer. The purpose was to see whether the miRNA quantities found in particular types of carriers were more useful in differentiating cancer patients from healthy individuals than the overall quantity recovered from serum.

Materials and Methods

Chemicals and biomaterials. Chemicals used in this study were listed in the Supporting Information. HDL and low-density lipoprotein (LDL) were purchased from CalBioChem (EMD Millipore, Billerica, MA). Trizol LS reagent, 3,3'-dioctadecyloxacarbocyanine perchlorate (DiO) and Total Exosome Isolation kit were purchased from Invitrogen (Life Technologies). MicroRNA standards were purchased from Integrated DNA Technologies (Coralville, IA). TaqMan MicroRNA Assays specific to each miRNA strand were purchased from Applied Biosystems (Life Technologies).

Serum samples. The serum sample used for exosome extraction and separation method optimization was the pooled healthy male serum from Sigma-Aldrich. The serum samples used in the distribution profile study were provided by our collaborators at the City of Hope Medical Center (Duarte, CA). They were obtained from voluntarily consenting patients (females) under institutional review board-approved protocols. Both breast cancer patients had infiltrating ductal carcinoma and were ER/PR/HER2-positive (ER-estrogen receptor; PR-progesterone receptor; HER2- human epidermal growth factor receptor).

Serum fractionation by AF4. An AF2000 system manufactured by Postnova Analytics (Salt Lake City, UT) was used in this study. The trapezoidal separation channel was 0.350 mm thick (thickness of the spacer), and its tip-to-tip length was 275 mm, with an inlet triangle width of 20 mm and an outlet width of 5 mm. The injection loop volume was 20 µL. The surface area of the accumulation wall was 3160 mm^2, which was made out of the regenerated cellulose ultrafiltration membrane (Postnova Analytics) with the molecular weight cutoff (MWCO) value of 10 kDa. The eluate exiting AF4 passed through a SPD-20A absorbance detector (Shimadzu) followed by a fraction collector (Bio-Rad). The running buffer for all samples was the 1×PBS mentioned above.

During serum fractionation, an initial focusing step of eight minutes was used, with the cross flow (the flow exiting the channel through the membrane wall) at 3.00 mL/min, tip flow (the flow entering the channel from the inlet) at 0.30 mL/min, and focus flow (a flow entering at a position further down from the inlet to focus the analyte into a narrow sample zone) at 3.00 mL/min. After focusing, there was a 1 minute transition period where the tip flow increased to 3.30 mL/min and the focus flow was reduced to zero. Afterwards, the tip flow was kept at 3.30 mL/min for five minutes, and was then reduced to 0.30 mL/min over the course of 15 minutes. In each case, the cross flow was reduced to keep the detector flow (the flow exiting the channel from the outlet) at 0.30 mL/min. A fraction collector (Bio-rad) was used to perform step-wise collection at every minute interval. These 1-min collections for each sample were then combined into 6 fractions, with fraction #1 (F1) containing the eluents collected from 6 to 9 min, F2 from 9 to 13 min, F3 from 13 to 16 min, F4 from 16 to 19 min, F5 from 19 to 23 min, and F6 from 23 to 28 min.

RNA and protein extraction from collected fractions. Each fraction was spiked with 0.31 fmol C. elegans miRNA, *cel-miR*-67, and subjected to phenol-chloroform extraction using the Trizol® LS reagent (Invitrogen). Each fraction was split into several ~ 450 μL aliquots, each aliquot homogenized with 1 mL Trizol LS reagent followed with the addition of 300 μL chloroform. After phase separation, the RNA-containing aqueous phase was mixed with RNA-grade glycogen and the RNAs were precipitated by isopropanol (IPA). The RNA pellet was washed once by 80% ethanol, dried, and then all pellets for the same fraction were combined before going through another round of IPA precipitation and ethanol wash. The fractions were then dried and stored at -20 °C until RT-qPCR analysis. The protein-containing organic faction

was precipitated using IPA and washed with 0.3 M guanidine hydrochloride in ethanol. After drying, the protein pellets were reconstituted in water.

MicroRNA analysis. To acquire sufficient miRNA amounts, two collections were carried out for each serum in each repeat. One collection was used to quantify *hsa-miR*-16, *miR*-191, *let*-7a, *miR*-17, *miR*-155, and *miR*-375, in which the miRNA pellets were reconstituted in 31 μL TE buffer. The other collection was for quantification of *hsa-miR*-21and *miR*-122; and reconstitution of the miRNA pellets was done in 16 μL. The *cel*-miR-67 spiked into each fraction before RNA extraction was used as an internal standard to correct for sample loss during extraction, and the absolute miRNA quantity in each sample was obtained using an external standard calibration curve prepared from reactions with standard miRNAs. Details of the RT-qPCR reaction conditions can be found in the Supporting Information.

Results and Discussion

AF4 separation of miRNA carriers. Due to the large differences in the hydrodynamic diameter (d_h) between proteins and exosomes, the AF4 separation condition needs to be optimized to elute all carriers in a reasonable period of time while maintaining modest resolution between different species. In particular, elution of large particles like exosomes could take a very long time, since their diffusion rate is slow. Under a constant channel/cross flow condition, the exosomes prepared by the Total Exosome Isolation kit (Supporting Information) was injected but not eluted within 30 minutes, unless the cross flow was turned off gradually (Supporting Information, **Figure S1a and b**). It turned out that better resolution between exosomes and the smaller serum components, as well as quick elution of the exosomes with limiting peak tailing,

was achieved if the cross flow gradually decreased to zero within 15 minutes (**Fig. S1c**). Using

this flow program, protein standards with various d_h: albumin (Mw 67 kDa, $d_h \sim 4$ nm), IgG (Mw

150 kDa, $d_h \sim 8$ nm) and thyroglobulin (Mw 660 kDa, $d_h \sim 16$ nm), as well as the polystyrene

nanoparticle ($d_h = 50 \pm 7$ nm, representing the average exosome diameter), were eluted at different

times (Supporting Information, **Figure S2a**); so did the HDL ($d_h \sim 7\sim10$ nm), LDL ($d_h \sim 21$-28

nm), and exosomes (**Figure S2b**). The results support that the major serum carriers could be

eluted in the order of single proteins < HDL < LDL < exosomes (ranking by elution time). To

further improve separation resolution between the larger lipoprotein particles and exosomes, a 5-

min constant flow period, i.e. the cross flow was maintained at 3.0 mL/min for 5 min before

starting to ramp down (**Figure S3**) was used. This condition also gave out slight improvement

when resolving the single proteins and HDL. This new method was then used in the subsequent

experiments.

The whole human serum purchased from Sigma was fractionated by the optimized AF4

method. We also spiked pure HDL and LDL to the serum for determination of their exact elution

windows (**Figure 1a**). HDL was eluted within 10-15 min and LDL between 17 and 23 min.

Moreover, we stained the serum or the exosome extracts with the lipophilic dye of DiO prior to

AF4 fractionation. DiO is weakly fluorescent in water, but emits strong fluorescence with high

photo-stability when incorporated into lipid membranes. The fractograms obtained with

fluorescence detection ($\lambda_{ex} = 490$ nm; λ_{em} at 510 nm) further confirmed that, structures with lipid

membranes were mainly eluted after 17 minutes (**Fig. 1b**).

Fractionation of patient serum and confirmation of carriers eluted in each fraction. Once

the approximate windows for elution of the known miRNA carriers were known, we fractionated

sera samples collected from 2 healthy females (**control**, referred as Control #1 and #2) and 2

breast cancer (BC) patients (**case**, Case #1 and #2) (**Figure 2**). Six fractions were collected to increase the purity of miRNA carriers enriched in each fraction. The collection window for each fraction was determined by the relative elution times of HDL, LDL, and exosomes obtained from the above study (inset table in **Fig. 2**). Separation was highly reproducible: relative standard deviation (RSD) of the elution time of the peak within each fraction was < 8% using all 8 fractograms collected (four serum samples, each with two repeats) (Supporting Information, **Figure S4a & c**). We also performed DiO staining for all the 4 serum samples tested, and confirmed the reproducible elution of the carriers with rich lipid structures, such as HDL, LDL, and exosomes (**Fig. S4b & d**). The highly reproducible separation profiles obtained by both UV absorption and DiO staining coupled with fluorescence detection helped to confirm the similarity in regular protein (represented by the peak intensity of serum albumin and IgG) and lipid (represented by the two major peaks detected by DiO staining) contents among these samples. This can ensure that the difference detected in miRNA distribution profiles was originated from the presence of BC but not from difference in carrier abundance. Moreover, the high reproducibility greatly simplified the after-column collection: a fraction collector was programmed to automatically collect the eluent every one minute, and the fractions within the desired time windows were combined for subsequent miRNA and protein extraction.

To confirm the identities of carriers enriched in each fraction, proteins eluted in F1-F6 were collected, digested by trypsin, and analyzed by LC-MS/MS. The relative abundance of the eluted proteins were evaluated by spectral counting,[44-46] which counts the number of mass spectra collected for a specific protein. The percentage of the spectra number for a particular protein among all spectra identified in one sample should be semi-quantitatively proportional to its relative abundance in the mixture.[47] Apolipoproteins belonging to various lipoprotein

complexes, such as apolipoprotein A-I (ApoA-I), A-II (ApoA-II) and B-100 (ApoB), were found in multiple fractions (Figure 3a). ApoA-I, as the marker for HDL, was found in F2-F6, probably because of its association with all lipoprotein complexes and even in exosomes. The other marker protein for HDL, ApoA-II, was present in F2-F4 fractions, and also more enriched in F3. Considering the size range of HDL reported in literature, i.e. 7~10 nm,[48] we concluded the heterogeneous high-density lipoprotein (HDL) particles were eluted in F2, F3, and F4. ApoB is the marker protein for LDL as well as the very-low-density lipoproteins (VLDL),[49] and was found in F4-F6, with the majority eluted in F5. Thus, LDL should be enriched in F5, matching with migration window of the pure LDL shown in Fig. S2b and Fig. 1a.

LC-MS/MS did not identify marker proteins for exosomes, probably due to the signal suppression resulted from the highly abundant serum proteins like IgG and albumin. Instead, we detected the marker protein for exosomes, CD-63, in each fraction by ELISA (Figure 3b). About 20 ng of the protein extracted from each fraction (determined through the bicinchoninic acid assay) was adsorbed to the bottom of the microtiter plate well. CD-63 was detected by the anti-CD63 antibody and the HRP-labeled secondary antibody. A substantial amount of CD63 (~6 ng/20 ng) was detected in F6. As was concluded from the standards analysis, F6 was where exosomes were primarily located.

Overall, the above results point out that, F1 contained mainly albumin or proteins with MW < 100 kDa. HDL and LDL should be enriched in F3 and F5, respectively; and exosomes mainly in F6, but could also be in F5. VLDL was co-eluted with exosomes in F6. Although co-elution of multiple carriers was seen using the current separation method, such as the overlap of HDL and LDL in F4, and the coelution of exosomes and VLDL in F6, enriching specific carriers in particular fractions should already allow us to look at the general distribution of miRNAs

among the carriers. Higher resolution will indeed enhance the accuracy in distribution profiling, and can be achieved by injecting lower amounts serum in each round of the separation, but multiple collections will be needed, increasing the overall labor in the analysis, which is not a favorable choice. Increasing the separation force by using a higher crossflow may also be beneficial to separation resolution, but we take the risk of losing more miRNAs due to membrane adsorption. Thus, we used the current fractionation conditions for the present work. Our results, as would be seen in the following discussion, showed that the coarse distribution profiles were adequate in differentiating the cancer patients from healthy controls, as well as in revealing strands and particular carriers that were important to the differentiation.

Distribution of miRNAs in serum. The total RNAs were precipitated and reconstituted in water for quantification by RT-PCR. As stated above, sera from two groups of donors (all females) were tested. The sera from healthy individuals (Control #1 and #2); and those from breast cancer patients (Case #1 and #2) were analyzed, each with two repeated measurements. Eight miRNAs were quantified by RT-qPCR. Their sequences are listed in **Table S1,** together with the rationale of their inclusion in our study.

Recovery of miRNAs in our method was evaluated by quantification of *miR-16* in the Sigma serum. The total content of *miR-16* directly extracted from the whole 20-µL serum by the TRIzol reagent was compared with the sum miRNA quantity recovered from all AF4 fractions obtained with the injection of the same serum volume. A recovery as high as 98% was achieved (Supporting Information, Figure S5), indicating no significant loss of miRNAs due to membrane adsorption inside the AF4 channel. The resulted copy number of each miRNA tested in 20-µL serum normally ranged from 10E4 to 10E10. *miR*-375 and -122 were present at much lower abundances than other strands or even not detected in some of the fractions.

The high reproducibility in the separation step and careful processing in miRNA extraction and quantification ensured high analytical reproducibility: the RSD for the Log value of the total miRNA content in the two repeated measurements was < 5% for most of the strands, except for *miR*-375, -21, and -122, which could vary by up to 15%. Agreed with previous reports, large variations in the miRNA amounts were observed among individuals, even between the two samples within the same health group: the controls or the BC cases. Evaluation of the RSD of the total miRNA amount in all serum samples points out that, *miR*-16 and -17 had relatively more stable expression among individuals than other miRNA species. Their RSD was below 15%. However, this RSD already corresponds to about 10-fold alteration in the miRNA copy numbers if the base value is around 10E6. For miR-122, RSD values close to 120% were observed between the two samples within the same group.

Since each fraction enriched a particular type of miRNA carrier, the copy number found in each fraction corresponded to the miRNA level in that particular carrier. Different miRNAs showed distinct distribution patterns among the carriers, as demonstrated by the distribution profile of Case #1 (**Figure 4a; the profiles of other samples were shown in Figure S6**). In this sample, higher amounts of *miR*-16, -17, and -122 were found in F4-F6. There was even no detectible *miR*-122 in F1-F3. Thus, these three miRNAs should mainly locate in lipoprotein complexes and exosomes in this serum sample. On contrary, *Let*-7a, *miR*-155, and *miR*-191 had quite flat distribution among all fractions. The main type of carriers for each miRNA could be related to the major pathway it takes when exiting the cells, and be possibly linked to their biological functions. By fractionating the carriers prior to miRNA quantification, our method provides rich information about how the miRNAs are present in serum, which can be further explored to solve the fundamentals of miRNA secretion and transportation.

We compared the miRNA copy number found in each fraction between the control and BC samples. **Figure 4b** shows the Log ratio of the averaged miRNA copy number in the BC samples over that in the control samples; i.e. Log (BC/control), for each miRNA. If the miRNA level was lower in the BC cases than in the controls, a negative Log(ratio) value would be obtained, and vice versa. Larger absolute values of Log (Case/Control) indicate more obvious difference between these two groups. We also included the Log(Case/Control) obtained using the total miRNA quantity from all fractions (displayed as red bars). The sum was to represent the result attainable with the standard approaches in miRNA study, in which the overall expression level of each miRNA is quantified. Fig. 4b clearly showed that, larger differences between the BC and control samples was observed in some fractions than in the sum value for all miRNAs tested, except for *miR*-155 and -191. This result hints that the miRNA quantity change in some of the carriers could be more sensitive in differentiating the cancer patients from healthy controls than the overall quantity in the whole serum. This speculation was actually supported by the following statistical analysis.

Statistical analysis of the miRNA distribution profiles. To see whether the distribution

---

Box 1:

$Y_{ijk} = \mu + b_i + b_{j(i)} + \varepsilon_{ijk}$, $i = 1,2$ (# of patient group), $j = 1,2$ (sample # in each group), $k = 1,2$ (replication)

b_i : effect of ith group (fixed, 1 for the control group, 2 for the BC case group)

$b_{j(i)}$: effect of jth sample in group i (random, 1(1) for Control #1, 2(1) for Control #2, 1(2) for Case #1, 2(2) for Case #2)

$b_{j(i)} \sim N(0, \sigma_b^2)$, $\varepsilon_{ijk} \sim N(0, \sigma^2)$, $b_{j(i)}$ and ε_{ijk} are independent

---

profile could tell the difference between healthy donors and BC patients, and whether more reliable miRNA biomarkers can be found, for the 8 miRNAs listed in Table S1, we fitted their quantities in each fraction in the linear mixed effects model shown in **Box 1**, using **R 3.0.2**. For a miRNA in a given fraction, Y is the log value of the observed miRNA copy number. For example, for *miR*-16 in F1, Y_{111} is the Log value of the miRNA copy number from one of the

two repeats of Control #1. This linear mixed effects model allows us to account for sample to sample variation σ_b^2, as well as within sample variation σ^2, when comparing healthy donors to BC patients, i.e., testing the hypothesis $H_0:b_1=b_2=0$. We tested this hypothesis for each fraction of each one of the eight miRNAs using likelihood ratio test. To compare with standard approach, the same test was also performed on the sum of all fractions for each miRNAs. More miRNA strands (*miR*-16, -17, -375, and -122) in particular fractions (*miR*-16 in F5 & F6, -17 in F4, -375 in F4, and -122 in F4) yielded significant difference between healthy donors and BC patients at the level of 0.05, as marked by the "*" sign in Fig. 4b; while only miR-16 and 17 showed significant difference if the sum value was used.

It is interesting to see that miRNA quantity in F4 or F6 seems to matter the most in differentiating cases from controls. While F6 mainly contained exosomes, F4 enriched HDL and LDL. Then it is possible that, while all four markers may be valuable in diagnosis of breast cancer, they may be released by cancer cells via different pathways. *miR*-16 could be secreted in exosomes; but *miR*-17, -375, and -122 in the lipoprotein complexes could be more relevant to the development breast cancer than the exosomal fraction. This highlights the necessity of testing the miRNA quantities in multiple carriers, instead of in only one.

To visualize the effectiveness of the quantity of *miR*-16 in F5 and F6; *miR*-17 in F4; *miR*-375 in F4, and *miR*-122 in F4, in discriminating healthy donors and BC patients, we performed principal component analysis (PCA) using XLSTAT 2014 (Addinsoft[TM]). The contents of each miRNA in individual fractions were considered as the variables. For example, the *miR*-16 content in F6 is one variable and named as *miR*-16-F6. A total of 8 observations were made in our study (two repeats for each sample were counted as two independent observations PCA suggests that the first principle component with loadings -0.436, -0.598,-0.167,-0.258, 0.599 on

miR-16-F5, *miR*-16-F6, 17-F4, 375-F4, and 122-F4, respectively, can potentially separate healthy donors from BC patients, as shown in the scores plot in Figure 4c. In fact, the first principle component already accounts for 87.1% total variation. Certainly, a sample set containing a much larger number of both healthy controls and cancer patients should be analyzed to draw affirmative conclusion about the capability of these potential markers in cancer diagnosis.

Conclusions

In this research, AF4 was used to rapidly and reproducibly separate serum into fractions, thereby enriching various types of miRNA carriers. Accurate quantification of the miRNA in each fraction yielded the distribution profile. Applying our method to study the miRNA distribution profiles in few number of clinical samples in this proof-of-principle study, we found that the quantity of some miRNAs in particular fractions exhibited more distinct difference between healthy individuals and BC patients, than the overall quantity. Our results indicate that, such miRNAs, when present in some type of carriers, could be more specific and sensitive biomarkers for cancer diagnosis. The knowledge of the carrier then could help to improve our understanding on the fundamentals behind differential secretion of the miRNA markers by cancer cells and their transportation pathways in the circulation system. Such information can help to interpret their functions, and help with discovery of more effective therapeutic approaches.

ASSOCIATED CONTENT

Supporting Information. Methods used for separation of standard proteins and particles, for protein identification by LC-MS/MS, for the process of RT-qPCR, and for the ELISA procedure in detection of CD-63 in fractions were included; the sequences and information of the selected miRNA strands used in this study were shown in Table S1; Fig. S1 contained the fractograms of exosome extract obtained during method optimization, and those for protein and carrier standards analysis were displayed in Fig. S2; fractograms for serum fractionation with or without a constant flow region at the beginning can be found Fig. S3; Fig. S4 displayed the fractograms obtained by UV absorption and fluorescence for all samples and repeats; Fig. S5 was the result of the recovery study; Fig. S6 showed the miRNA profiles of the two controls and Case #2. This material is available free of charge via the Internet at http://pubs.acs.org.

AUTHOR INFORMATION

Corresponding Author

Dr. Wenwan Zhong, Department of Chemistry, University of California, Riverside, CA 92521-0403, USA

Email: wenwan.zhong@ucr.edu; Tel : 951-827-4925 ; Fax: 951-827-4713

Author Contributions

The manuscript was written through contributions of all authors. All authors have given approval to the final version of the manuscript.

‡These authors contributed equally.

ACKNOWLEDGMENT

REFERENCES

(1)   Chowdhury, D.; Choi, Y. E. and Brault, M. E. *Nat. Rev. Mol. Cell Biol.* **2013**, *14*, 181-189.

(2)   Wahlestedt, C. *Nat. Rev. Drug Discovery* **2013**, *12*, 433-440.

(3)   Hagen, J. W. and Lai, E. C. *Cell Cycle* **2008**, *7*, 2327-2332.

(4)   Nicoloso, M. S.; Spizzo, R.; Shimizu, M.; Rossi, S. and Calin, G. A. *Nat. Rev. Cancer* **2009**, *9*, 293-302.

(5)   Shi, M.; Liu, D.; Duan, H.; Shen, B. and Guo, N. *Cancer Metastasis Rev.* **2010**, *29*, 785-799.

(6)   Volinia, S.; Galasso, M.; Costinean, S.; Tagliavini, L.; Gamberoni, G.; Drusco, A.; Marchesini, J.; Mascellani, N.; Sana, M. E.; Abu Jarour, R.; Desponts, C.; Teitell, M.; Baffa, R.; Aqeilan, R.; Iorio, M. V.; Taccioli, C.; Garzon, R.; Di Leva, G.; Fabbri, M.; Catozzi, M.; Previati, M.; Ambs, S.; Palumbo, T.; Garofalo, M.; Veronese, A.; Bottoni, A.; Gasparini, P.; Harris, C. C.; Visone, R.; Pekarsky, Y.; de la Chapelle, A.; Bloomston, M.; Dillhoff, M.; Rassenti, L. Z.; Kipps, T. J.; Huebner, K.; Pichiorri, F.; Lenze, D.; Cairo, S.; Buendia, M.-A.; Pineau, P.; Dejean, A.; Zanesi, N.; Rossi, S.; Calin, G. A.; Liu, C.-G.; Palatini, J.; Negrini, M.; Vecchione, A.; Rosenberg, A. and Croce, C. M. *Genome Res.* **2010**, *20*, 589-599.

(7)   Dontu, G. and de Rinaldis, E. *Breast Cancer Res.* **2009**, *12*, 301.

(8)   Ma, L. and Weinberg, R. A. *Trends Genet.* **2008**, *24*, 448-456.

(9)   Ventura, A. and Jacks, T. *Cell* **2009**, *136*, 586-591.

(10)   Creemers, E. E.; Tijsen, A. J. and Pinto, Y. M. *Circ. Res.* **2012**, *110*, 483-495.

(11)   Lagana, A.; Russo, F.; Veneziano, D.; Di Bella, S.; Giugno, R.; Pulvirenti, A.; Croce, C. M. and Ferro, A. *Front. Non-Coding RNA* **2013**, *4*, 120.

(12)   Olivieri, F.; Rippo, M. R.; Procopio, A. D. and Fazioli, F. *Front. Non-Coding RNA* **2013**, *4*, 121.

(13)   Rykova, E. Y.; Laktionov, P. P. and Vlassov, V. V. *Nucleic Acids Mol. Biol.* **2010**, *25*, 93-128.

(14)   Williams, Z.; Ben-Dov, I. Z.; Elias, R.; Mihailovic, A.; Brown, M.; Rosenwaks, Z. and Tuschl, T. *Proc. Natl. Acad. Sci. USA* **2013**, *110*, 4255-4260.

(15)   Mitchell, P. S.; Parkin, R. K.; Kroh, E. M.; Fritz, B. R.; Wyman, S. K.; Pogosova-Agadjanyan, E. L.; Peterson, A. and Tewari, M. *Proc. Natl. Acad. Sci. USA.* **2008**, *105*, 10513-10518.

(16)   Russo, F.; Di Bella, S.; Nigita, G.; Macca, V.; Lagana, A.; Giugno, R.; Pulvirenti, A. and Ferro, A. *PLoS One* **2012**, *7*, e47786.

(17)   Wu, X.; Somlo, G.; Yu, Y.; Palomares, M. R.; Li, A. X.; Zhou, W.; Chow, A.; Yen, Y.; Rossi, J. J.; Gao, H.; Wang, J.; Yuan, Y.-C.; Frankel, P.; Li, S.; Ashing-Giwa, K. T.; Sun, G.; Wang, Y.; Smith, R.; Robinson, K.; Ren, X. and Wang, S. E. *J. Translational Med.* **2012**, *10*, 42.

(18)   Samantarrai, D.; Dash, S.; Chhetri, B. and Mallick, B. *Mol. Cancer Res.* **2013**, *11*, 315-328.

(19)   Arroyo, J. D.; Chevillet, J. R.; Kroh, E. M.; Ruf, I. K.; Pritchard, C. C.; Gibson, D. F.; Mitchell, P. S.; Bennett, C. F.; Pogosova-Agadjanyan, E. L.; Stirewalt, D. L.; Tait, J. F. and Tewari, M. *Proc. Natl. Acad. Sci. USA* **2011**, *108*, 5003-5008, S5003/5001-S5003/5019.

(20)   Li, L.; Zhu, D.; Huang, L.; Zhang, J.; Bian, Z.; Chen, X.; Liu, Y.; Zhang, C.-Y. and Zen, K. *PLoS One* **2012**, *7*, e46957.

(21)   Vickers, K. C.; Palmisano, B. T.; Shoucri, B. M.; Shamburek, R. D. and Remaley, A. T. *Nat. Cell Biol.* **2011**, *13*, 423-433.

(22)   Vickers, K. C. and Remaley, A. T. *Curr. Opin. Lipidol.* **2012**, *23*, 91-97.

(23)   Diehl, P.; Fricke, A.; Sander, L.; Stamm, J.; Bassler, N.; Htun, N.; Ziemann, M.; Helbing, T.; El-Osta, A.; Jowett, J. B. M. and Peter, K. *Cardiovasc. Res.***2012**, *93*, 633-644.

(24)   Xu, J.; Chen, Q.; Ke, Z.; Zhang, C. and Zhang, Q. *J. Neurochem.* **2013**, *124*, 15-25.

(25)   Yang, M.; Chen, J.; Su, F.; Yu, B.; Su, F.; Lin, L.; Liu, Y.; Huang, J.-D. and Song, E. *Mol. Cancer* **2011**, *10*, 117.

(26)   Palma, J.; Yaddanapudi, S. C.; Pigati, L.; Havens, M. A.; Jeong, S.; Weiner, G. A.; Weimer, K. M. E.; Stern, B.; Hastings, M. L. and Duelli, D. M. *Nucleic Acids Res.* **2012**, *40*, 9125-9138.

(27)   Kosaka, N. *J.Biol. Chem.***2010**, *285*, e99946.

(28)   Kosaka, N.; Iguchi, H.; Yoshioka, Y.; Hagiwara, K.; Takeshita, F. and Ochiya, T. *J. Biol. Chem.* **2012**, *287*, 1397-1405.

(29)   Umezu, T.; Ohyashiki, K.; Kuroda, M. and Ohyashiki, J. H. *Oncogene* **2013**, *32*, 2747-2755.

(30)   Gallo, A.; Tandon, M.; Alevizos, I. and Illei, G. G. *PLoS One* **2012**, *7*, e30679.

(31)   Turchinovich, A.; Weiz, L.; Langheinz, A. and Burwinkel, B. *Nucleic Acids Res.* **2011**, *39*, 7223-7233.

(32)   Zhou, W.; Fong, M. Y.; Min, Y.; Somlo, G.; Liu, L.; Palomares, M. R.; Yu, Y.; Chow, A.; Timothy, S.; Connor, F. O.; Chin, A. R.; Yen, Y.; Wang, Y.; Marcusson, E. G.; Chu, P.; Wu, J.; Wu, X.; Li, A. X.; Li, Z.; Gao, H.; Ren, X.; Boldin, M. P.; Lin, P. C. and Wang, S. E. *Cancer Cell* **2014**, *25*, 501-515.

(33)   Yoo, C. E.; Kim, G.; Kim, M.; Park, D.; Kang, H. J.; Lee, M. and Huh, N. *Anal. Biochem.***2012**, *431*, 96-98.

(34)   Mathivanan, S.; Lim, J. W. E.; Tauro, B. J.; Ji, H.; Moritz, R. L. and Simpson, R. J. *Mol. Cell. Proteomics* **2010**, *9*, 197-208.

(35)   Tauro, B. J.; Greening, D. W.; Mathias, R. A.; Ji, H.; Mathivanan, S.; Scott, A. M. and Simpson, R. J. *Methods* **2012**, *56*, 293-304.

(36)   Yamada, T.; Inoshima, Y.; Matsuda, T. and Ishiguro, N. *J. Veterinary Med. Sci.* **2012**, *74*, 1523-1525.

(37)   Wahlund, K. G. and Giddings, J. C. *Anal.Chem.***1987**, *59*, 1332-1339.

(38)   Madorin, M.; van Hoogevest, P.; Hilfiker, R.; Langwost, B.; Kresbach, G. M.; Ehrat, M. and Leuenberger, H. *Pharm. Res.* **1997**, *14*, 1706-1712.

(39)   Pollastrini, J.; Dillon, T. M.; Bondarenko, P. and Chou, R. Y. T. *Anal. Biochem.* **2011**, *414*, 88-98.

(40)   Schachermeyer, S.; Ashby, J. and Zhong, W. W. *J. Chromatogr. A* **2013**, *1295*, 107-113.

(41)   Kim, K. H. and Moon, M. H. *Anal. Chem.* **2011**, *83*, 8652-8658.

(42)   Oh, S.; Kang, D. J.; Ahn, S. M.; Simpson, R. J.; Lee, B. H. and Moon, M. H. *J. Sep. Sci.* **2007**, *30*, 1082-1087.

(43)   Yang, I.; Kim, K. H.; Lee, J. Y. and Moon, M. H. *J. Chromatogr. A* **2014**, *1324*, 224-230.

(44)   Chien, K.-y. and Goshe, M. B. *Curr. Anal.Chem.* **2009**, *5*, 166-185.

(45)　　Neilson, K. A.; Ali, N. A.; Muralidharan, S.; Mirzaei, M.; Mariani, M.; Assadourian, G.; Lee, A.; van Sluyter, S. C. and Haynes, P. A. *Proteomics* **2011**, *11*, 535-553.

(46)　　Zhu, W.; Smith, J. W. and Huang, C.-M. *J. Biomed. Biotechnol.* **2010**, No pp given.

(47)　　Zhou, W.; Liotta, L. A. and Petricoin, E. F. *Cancer Genomics Proteomics* **2012**, *9*, 135-142.

(48)　　Camont, L.; Chapman, M. J. and Kontush, A. *Trends Mol. Med.* **2011**, *17*, 594-603.

(49)　　Kim, K. H.; Lee, J. Y.; Lim, S. and Moon, M. H. *J. Chromatogr. A* **2013**, *1280*, 92-97.

Captions for Tables and Figures:

Figure 1 – A) Fractograms (UV absorption at 280 nm) for serum before and after spiked with HDL or LDL. B) Comparison of fractograms (detected by fluorescence with 480ex/510em) of serum and exosome extract after DiO staining.

Figure 2 – Fractograms for serum samples from healthy individuals (controls) and BC patients (cases). The table shows the time range of each collected fraction; and the RSD values of the peak elution time for each fraction. N/A means no distinct peak in the fraction.

Figure 3 – A) Spectral counting results for selected lipoproteins in the AF4 fractions. B) ELISA detection of CD-63 in the collected fractions.

Figure 4 – A) The distribution profiles of the 8 tested miRNAs in the serum collected from one breast cancer patient (Case #1). B) Change in the averaged Log value of miRNA copies (counting all four tests – 2 samples with 2 repeats–in each group) between the controls and cases. "*" marked out those showing significant difference between healthy donors (controls) and BC patients (cases) with $p < 0.05$. C) The score plot of principle component 1 vs. principle component 2 obtained by PCA on the miRNA quantity of miR-16, -17, -375, and -122 in certain fractions as indicated in the text. The arbitrary circles illustrated the separation between the control and case groups.
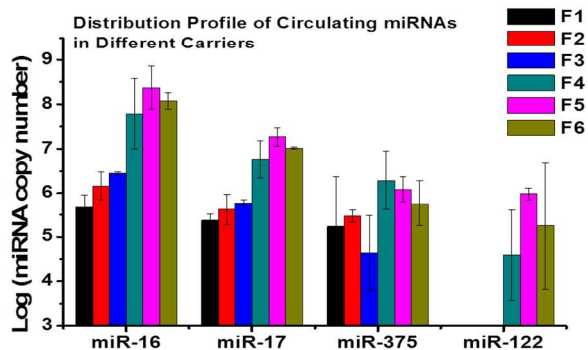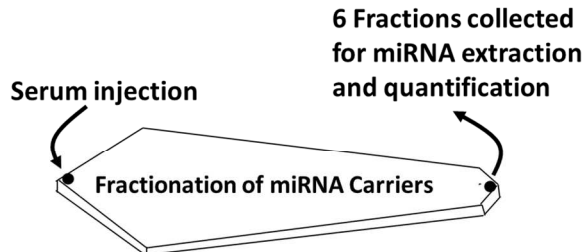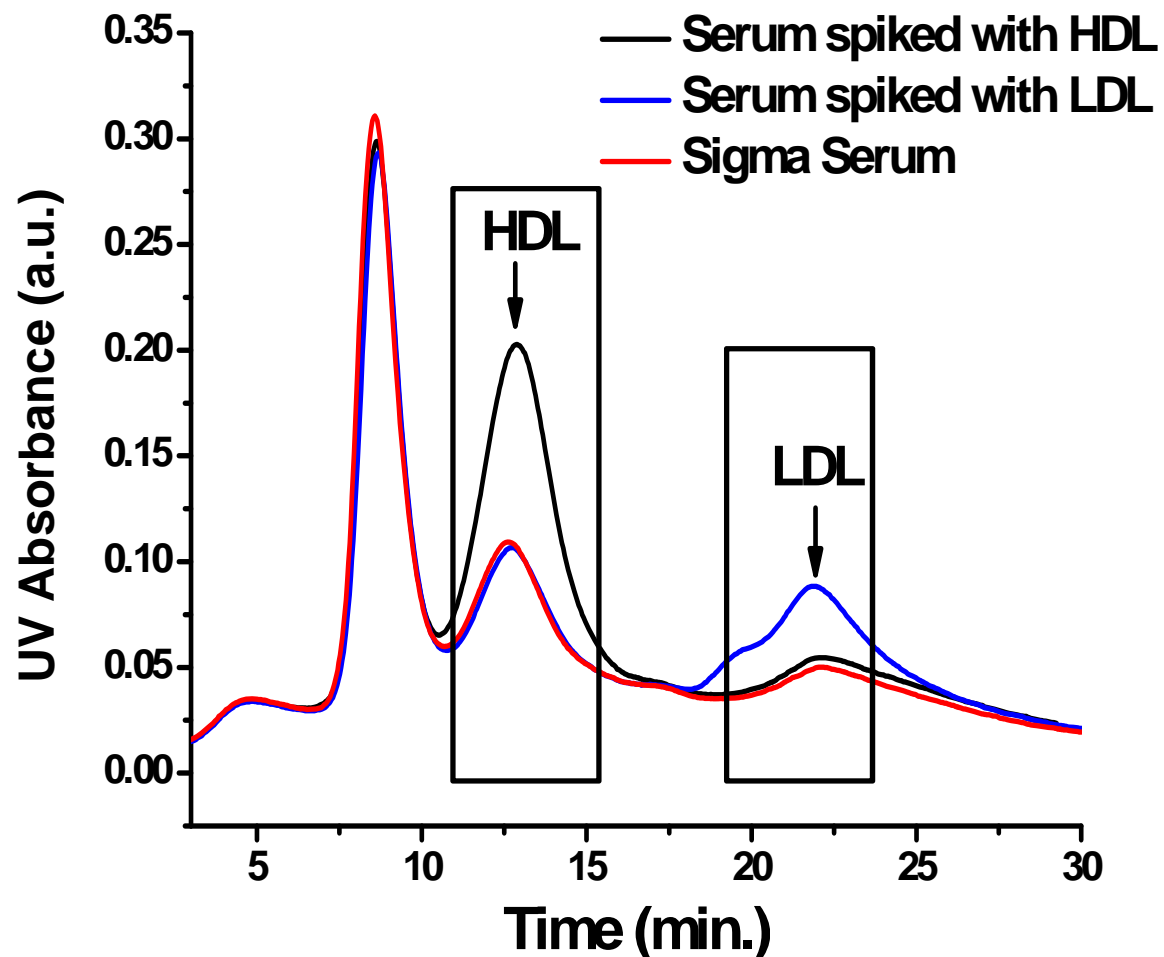
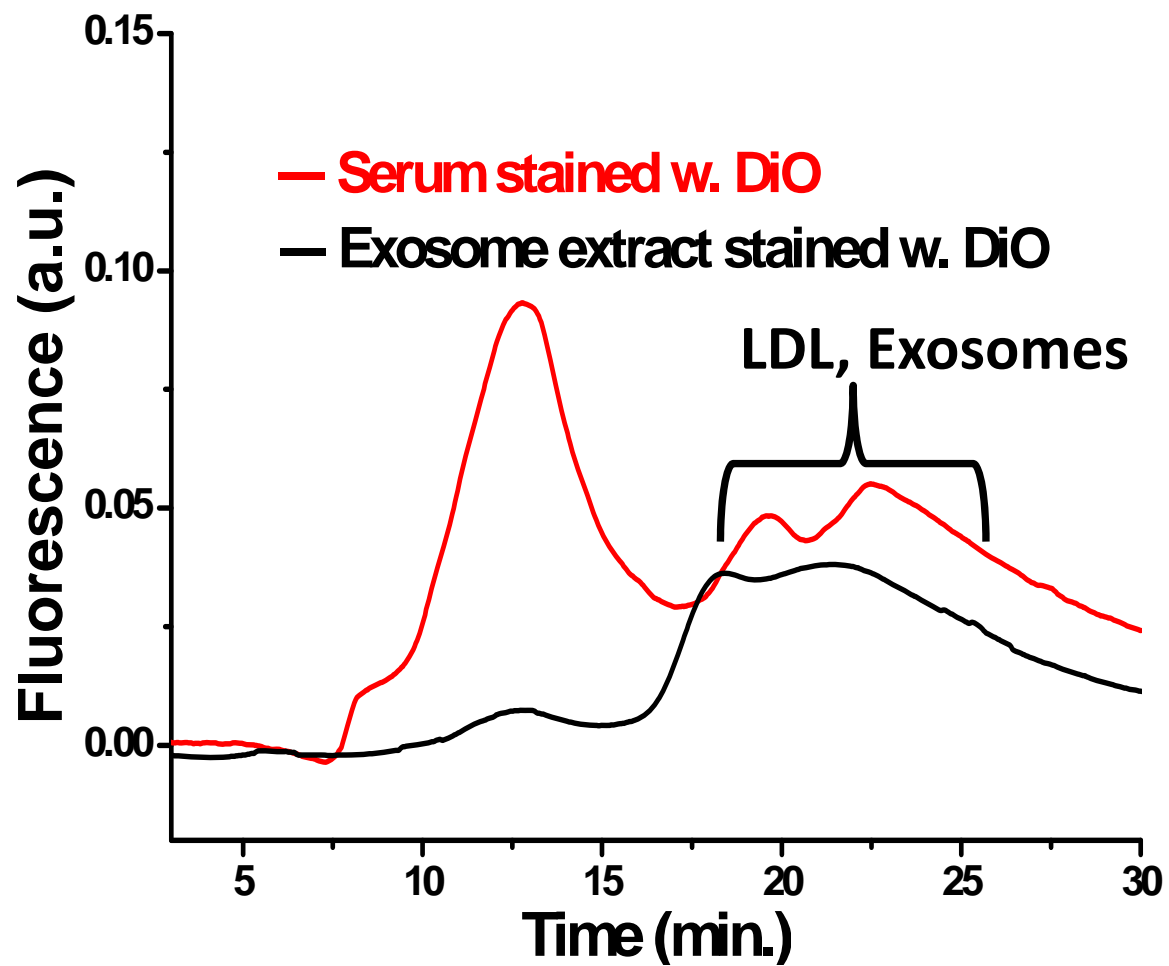**Table of Contents (TOC) Figure:**

Figure 1a

Figure 1b

Figure 2

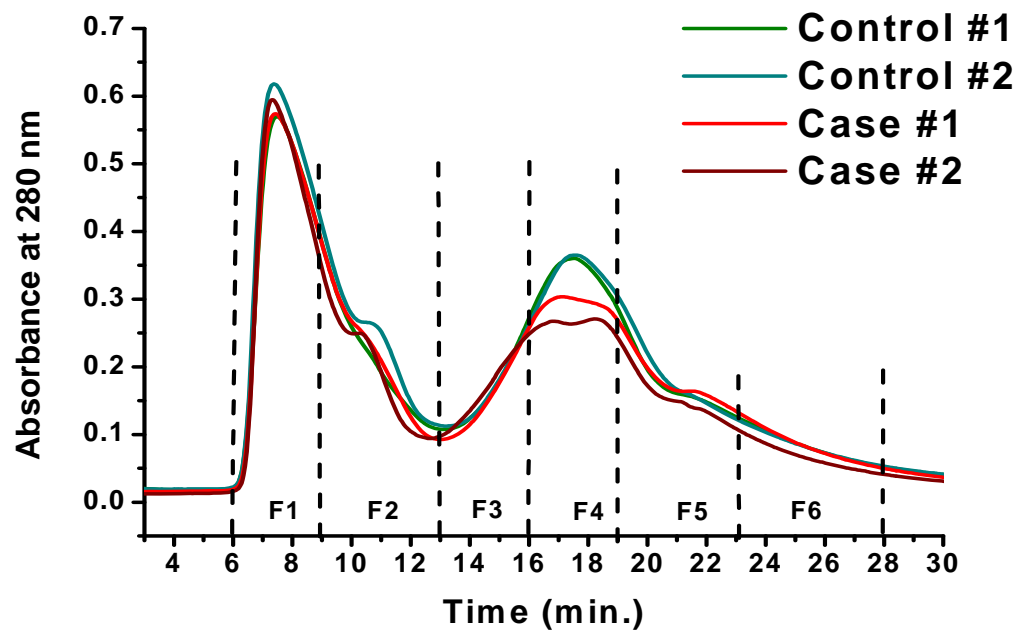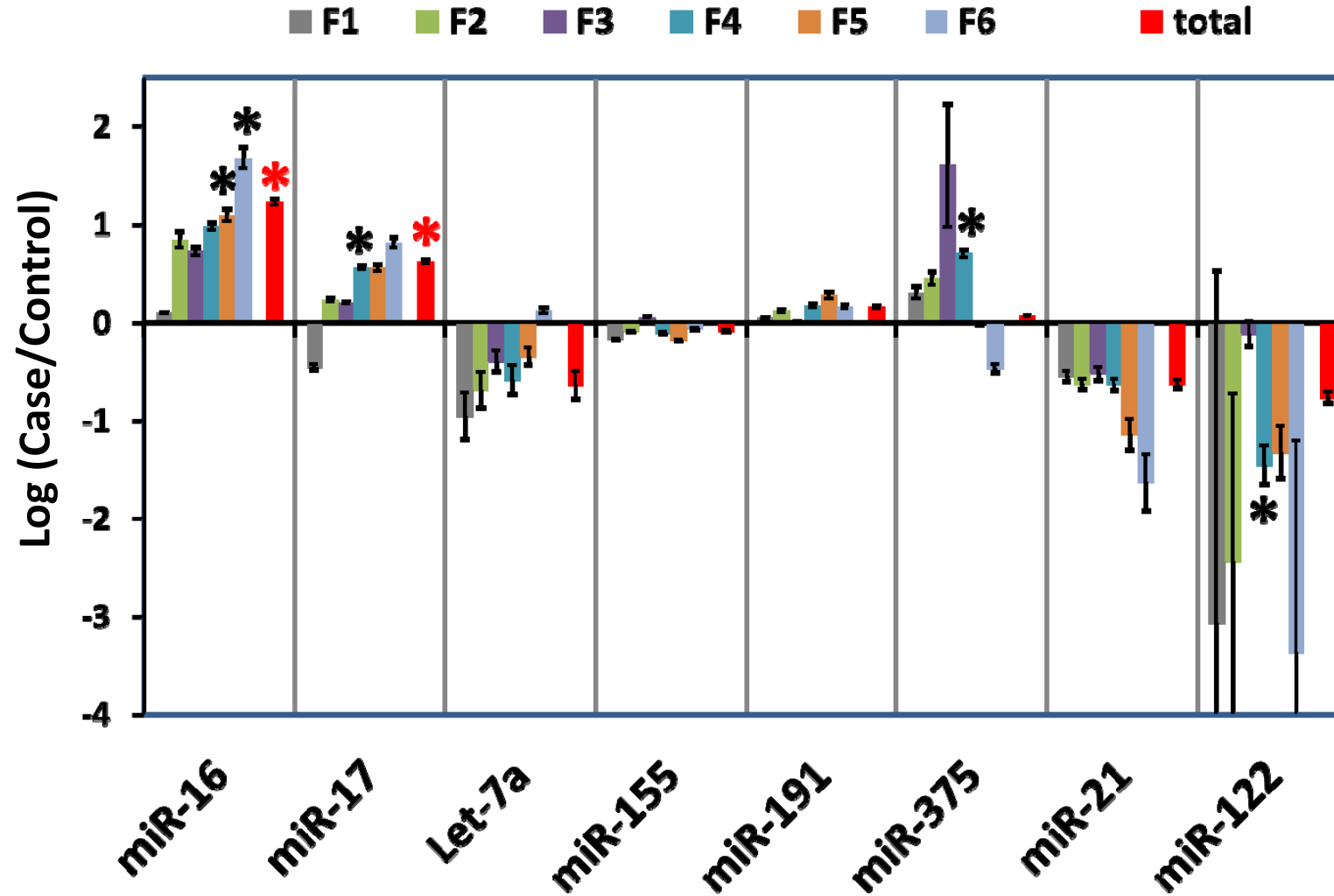| Fraction #	F1	F2	F3	F4	F5	F6
Fraction time range	6-9 min	9-13 min	13-16 min	16-19 min	19-23 min	23-28 min
RSD of peak elution time	8.0%	7.0%	N/A	4.4%	0.77%	N/A
Carrier (known or potential) enrichment	Single proteins, mainly albumin	HDL	HDL	HDL	LDL	Exosomes

Figure 3a
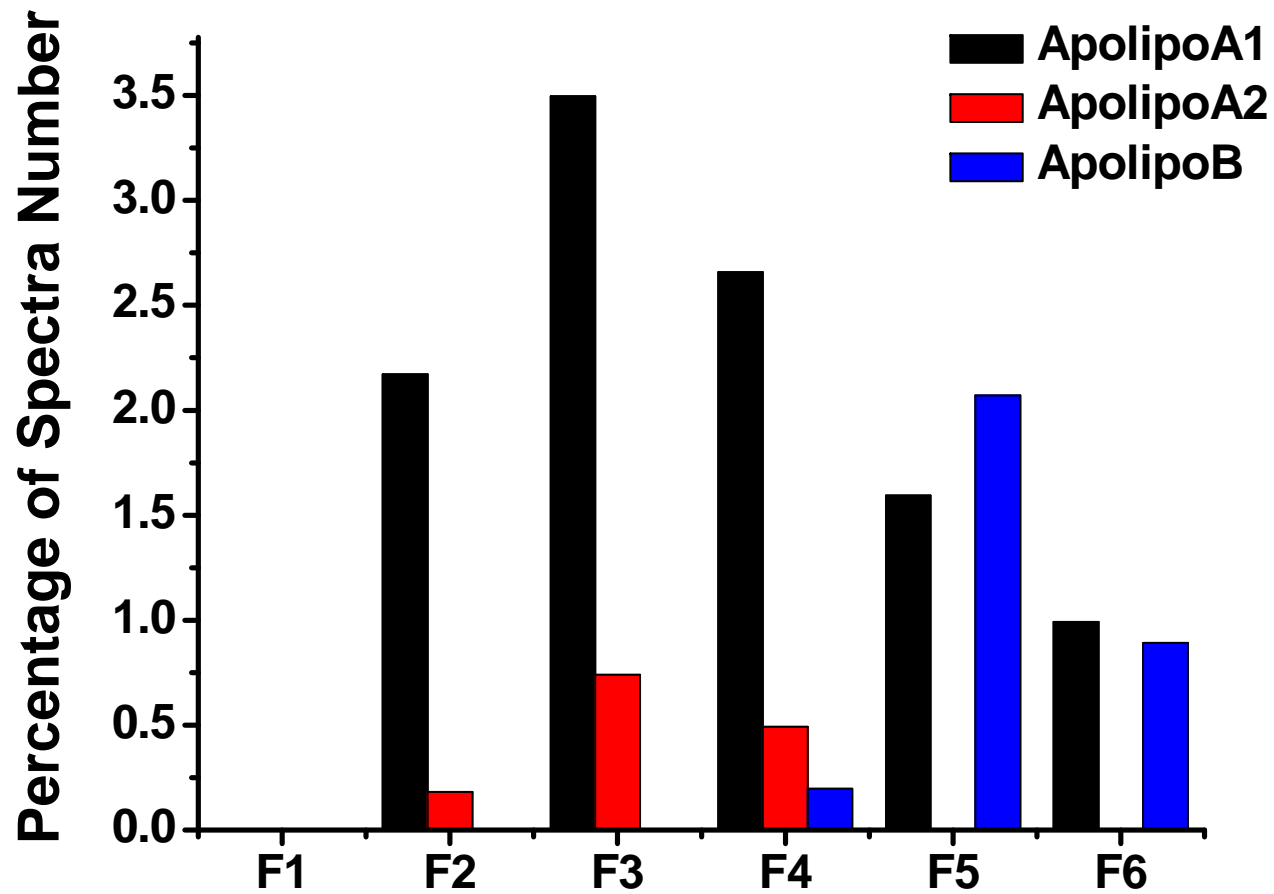
Figure 3b
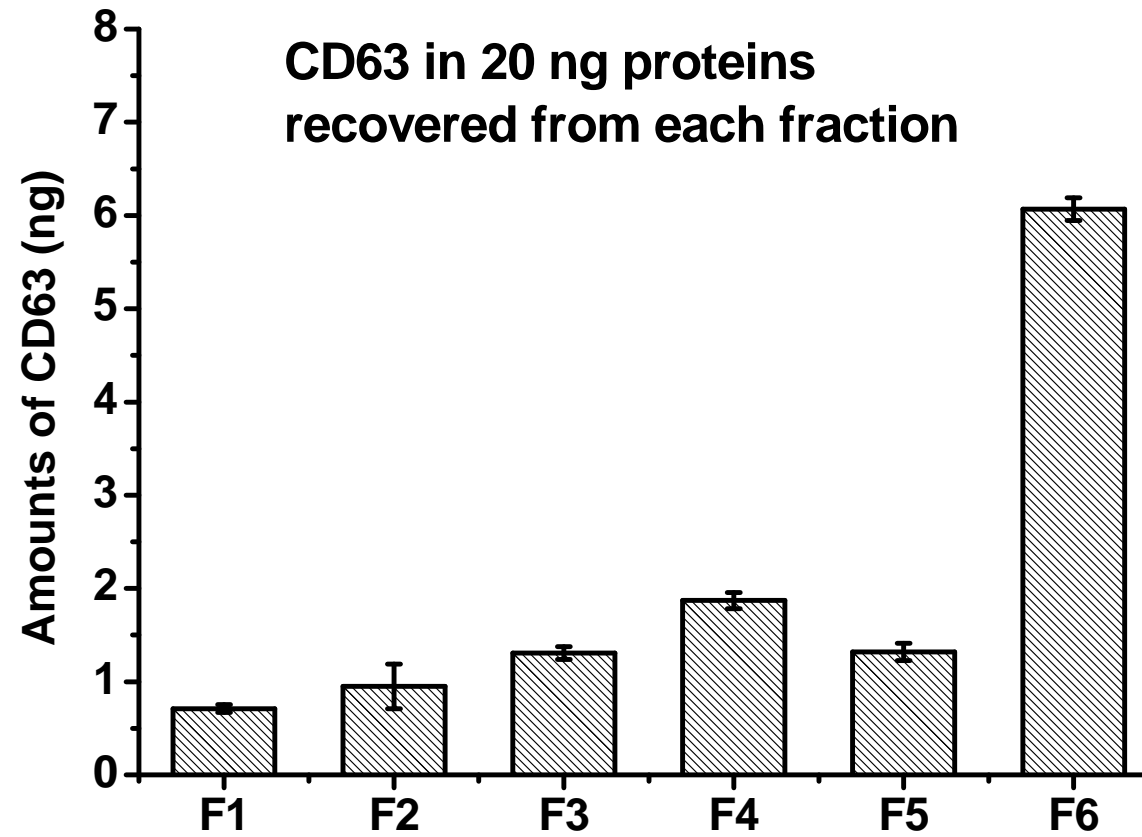
Figure 4a

Figure 4b

Figure 4c